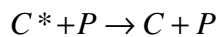
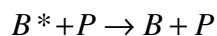
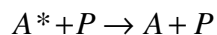
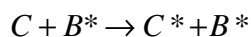
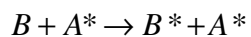
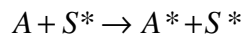


SI Text

Parameter Choices

We simulated a system consisting of 200 A (MAPKKK) species, 200 B species (MAPKK), and 1,000 C species (MAPK) and 600 generic phosphatases. Scaffold proteins are modeled as structural elements and are represented as rigid, immobile objects with each unit occupying one lattice site. Scaffolds do not change the activation energies for phosphorylation reactions and catalytic steps when species are bound to the scaffold. Each unit contains a binding site that is specific to a particular type of kinase and occupies one site on the lattice. We allow both inactive and active kinases to potentially bind to their specified binding sites and catalysis to take place when two appropriate species come into contact.

The reaction network was modeled in the simplest possible way by considering each elementary reaction event to comprise of a single reactive, thermally-active collision. The reactions used were:



Each reaction occurs in solution and when bound to the scaffold. Each species also can bind to and unbind from the scaffold, allowing for 27 possible chemical states of signaling complexes.

The energy barrier for association is zero, $E_2 = 0$, implying that proteins will bind to the scaffold when in contact with their selective binding sites. E , the energy barrier for disassociation from the scaffold, can range from 0 to 20. Note, for $E = 0$, statistically no

proteins are bound to the scaffold, and for $E = 20$, each binding site on a scaffold is occupied (on average) provided enough kinases are present. For simplicity, we consider the association and disassociation constants for each site on the scaffold to be the same unless otherwise noted. The energy barrier for activating a species by the appropriate kinase, E_3 , is taken to be zero, implying that phosphorylation will occur when an activated kinase collides with its appropriate substrate. E_4 , the energy barrier for deactivating a kinase, varies in the simulation trials and can take on values ranging from 0 to 10. For high phosphatase activity (i.e., a cascade that is intrinsically difficult to activate), $E_4 = 0$. For low phosphatase activity (i.e., a cascade that is intrinsically easy to activate), $E_4 = 6$. It is important to note that varying the number of phosphatases would have similar effects as varying E_4 . In this regard, E_4 then sets a basal level of phosphatase activity. For the case of a low signal, σ is taken to be 0.01. For the case of a high signal, σ is taken to be 1.0 or 0.25 as specified. ξ is set at 1, corresponding to one stoichiometric equivalent with respect to the first kinase in the cascade. Unless noted otherwise, all parameters used in particular simulations are those given above. But, we also studied the sensitivity of our results to variations in parameters.

Signaling in the Cytosol vs. a Membrane

We considered all events to occur in the cytosol. However, it has been shown that the MAPK cascade can become active in the course of membrane-proximal signaling events with a scaffold protein, such as KSR, being recruited to the plasma membrane. Also in some cases, scaffold-mediated signaling may be confined to the membranes of endosomes. Considering the signaling cascade on a plasma membrane does not change the qualitative results obtained from the simulations. The quantitative behavior of the signaling cascade, however, changes.

The effects that we report (i.e., amplification vs. attenuation) become, in some cases, more pronounced when signal transduction occurs on a membrane such as the plasma or nuclear membrane. Differences in the quantitative behavior follow from the following effects: the mobility of proteins in the plasma membrane is significantly smaller than for

proteins in the cytosol, and so the area that an active kinase can sweep out becomes smaller in two dimensions; also, the time it takes for a phosphatase to deactivate a kinase changes accordingly. A very interesting recent study (1) reports some of these effects in a scaffolded mammalian MAPK system. That study finds that the sensitivity of the MAPK pathway greatly increases when signaling is confined on a membrane.

Importance of Protein Diffusion

An important variable that determines the role of scaffolding a kinase cascade is the amount of time required (τ_{ec}) for an active kinase to encounter its downstream target. For simple diffusion, in three dimensions, $\tau_{ec} \sim \frac{1}{DC^{2/3}}$, where D is the diffusion constant and C is a typical concentration of kinases. Experiments indicate that τ_{ec} is significantly larger than $1 \mu\text{s}$ (on the order of 10^{-4} s to 10^0 s) (2). Our studies focused on these experimentally relevant conditions.

Monte Carlo time can be related to real time by equating a diffusion constant of a typical protein in the cytoplasm (i.e., $10 \mu\text{m}^2/\text{s}$) (2) with the diffusion constant used in most of our simulations [$1 (\text{lattice spacings})^2/\text{mcstep}$], and taking a value of the lattice spacing to be 10 nm. The cell is considered to have a $\sim 6\text{-}\mu\text{m}$ radius. This leads to a conversion factor, $1 \text{ mcstep} \sim 1 \mu\text{s}$. Typical physiological values of τ_{ec} range from $\sim 10^{-4}$ s to 1 s. These values are obtained from consideration of typical values of D (for a $\sim 50\text{-kDa}$ protein) in the cytoplasm ($10 \mu\text{m}^2/\text{s}$) and upper and lower bounds of kinase concentrations (3, 4). SI Fig. 7 gives an example of how protein mobility can influence the role of scaffold-mediated signal transduction.

Variations in Kinases Concentration and Catalytic Rates and Mechanisms

SI Fig. 6 illustrates some of the dependence of the results on kinase numbers and catalytic rates. We also explored the effects of incorporating enzymatic mechanisms for kinase activation rather than single reactive collisions. Specifically, we studied the following

mechanism: $E + S \xrightleftharpoons[k_{-1}]{k_1} ES \xrightarrow{k_{cat}} E + P$, where E is the enzyme, ES the enzyme-substrate

complex, and P is the product. The constants k_1 , k_{-1} , and k_{cat} , determine the kinetics. The rate of each elementary step is determined by an energy barrier. Qualitative results do not change for the parameter ranges used (SI Fig. 6 *e* and *f*). Energy barriers have been varied between 0 and $4 k_B T$ except for the catalysis step for the phosphatase inactivating a kinase that was varied from 0 to $8 k_B T$. Note that changes in energy barriers alter the effective rate constants exponentially, $k \sim e^{-(E/k_B T)}$, so our parameter variations change the rates by factors of ~ 50 and $\sim 3,000$ as the energy barriers are changed by 4 and $8 k_B T$, respectively. The insensitivity of our results to such large variations comes from the fact that these parameter choices do not limit the availability of the enzyme. Note that the effects of enzyme saturation (5) and distributive phosphorylation (6) have not been investigated.

Computation of Ensemble-Averaged Quantities

All calculations presented are carried out at steady state, and ensemble-averaged quantities are reported. Ensemble averaging was performed by first allowing the system to approach steady state as determined by no time dependence in the mean square

displacement, $\frac{d \langle [R(t) - R(0)]^2 \rangle}{dt} = 0$, and also ensuring that the simulation has

advanced to where the time is much longer than the reaction time scales; sampling of each configuration is done thereon. Simulations are carried out for $\sim 10^9$ Monte Carlo steps, a time much longer than the time to approach steady state and a time needed to acquire adequate statistics. These extended Monte Carlo trajectories ensure that there are no artifacts in our calculations because of insufficient statistical sampling. Analysis of the Monte Carlo trajectories shows that the approach to steady state is monotonic and that the results obtained are independent of initial conditions provided that the scaffolds are uniformly distributed within the simulation box. This indicates that the approach to steady state will also have the same properties as those reported for the steady-state

ensemble-averaged quantities. Thus, dynamical properties of the signaling cascade can be inferred from the steady-state distributions that we calculate.

Computer code for the kinetic Monte Carlo simulations was written in ANSI C and compiled with the GNU C Compiler. Simulations were carried out with serially clustered AMD Opteron 248 Processors. All data analysis was performed either with MATLAB or code written in the PERL scripting language.

Why Ordinary Differential Equations (ODEs) Were Not Used

The most commonly used method for modeling cell signaling dynamics is to use a set of ODEs and impose mass-action kinetic laws that govern the reaction dynamics subject to a prescribed network topology. It is therefore important to note that a model of scaffold-mediated signal transduction, based on ODEs and mass action kinetics, cannot capture the physical effects of the scaffolding revealed by our studies. As discussed in the text, scaffold proteins impose a stoichiometric constraint on how many downstream targets with which an activated kinase can interact. As shown before in many contexts (e.g., refs. 7 and 8), stoichiometric constraints introduce a length scale (L_{scaf} in our case). An ODE-based model using the “well-stirred chemical reactor approximation” (9), on the other hand, is a model with infinite ranged interactions and no length scales. Scenarios exist (e.g., low phosphatases levels in our model) where the ODE model would predict that scaffolds enhance signal transduction when this is physically impossible because of the inhibitory effects of the spatial constraints imposed by the stoichiometric limitation.

A Possible Model Based on Partial Differential Equations (PDEs)

We note that a different type of mean-field model involving a set of partial differential equations could conceivably capture the physical effects contained in the kinetic Monte Carlo simulations provided that the kinase concentration fields are properly constrained in the model. This approach would involve the numerical solution of many coupled

nonlinear PDEs. It may be interesting to investigate the qualitative behavior of a minimal model of this sort.

For an example, in a system with N scaffolds, and reactions characterized by kinetic parameters, k_+ (rate of phosphorylation), k_- (rate of dephosphorylation), k_{on} (rate of binding to the scaffold), k_{off} (disassociation rate for unbinding from the scaffold), and D (a protein diffusion coefficient), a set of reaction-diffusion equations can be constructed for the time evolution of the concentration of the i th activated species (denoted in the superscript), $\rho_u^{*i}(r, t)$, where $*$ indicates an activated kinase and the subscripts b and u identify a bound or unbound form of the molecule.

$$\frac{\partial \rho_u^{*i}(r, t)}{\partial t} = D \nabla^2 \rho_u^{*i}(r, t) + k_+ \rho_u^{*(i-1)}(r, t) \rho_u^i(r, t) - k_- \rho_u^{*i}(r, t) - \sum_{j=1}^N \delta(r - r_j) [k_{on} \rho_u^{*i}(r, t) \Theta(\rho^T - \rho_b^{*i}(r_j, t) - \rho_b^i(r_j, t)) - k_{off} \rho_b^{*i}(r, t)]$$

$$\frac{\partial \rho_b^{*i}(r, t)}{\partial t} = \sum_{j=1}^N \delta(r - r_j) \left[k_{on} \rho_u^{*i}(r, t) \Theta(\rho^T - \rho_b^{*i}(r_j, t) - \rho_b^i(r_j, t)) - k_{off} \rho_b^{*i}(r, t) + k_+ \rho_b^{*(i-1)}(r, t) \rho_b^i(r, t) - k_- \rho_b^{*i}(r, t) \right]$$

where r_j is the location of the j th scaffold, $\delta(r)$ is the Dirac delta function that confines each scaffold to a point in space, r , and the Heaviside step function, $\Theta(X)$ (defined as 0 for $X < 0$ and 1 for $X > 0$), imposes the constraint that the total concentration of a particular kinase $\rho_b^i(r, t) + \rho_b^{*i}(r, t)$ can accumulate at each scaffold site at r_j only up to a threshold value, ρ^T .

In such a phenomenological model, the time evolution of kinase concentration fields is set by incorporating diffusion, activation by a downstream kinases, deactivation, binding and unbinding to the scaffold, and inactivation and deactivation on the scaffold.

Influence of the Network of Interactions Between Phosphatases and Their Target Kinases

We investigated two distinct hypotheses. In SI Fig. 9 *a* and *b*, results are shown for cases in which a particular kinase can be inactivated in solution by a phosphatase but is protected from such deactivation when bound to the scaffold. SI Fig. 9 *c* and *d* shows results from simulations in which a particular kinase is protected from phosphatase-mediated deactivation (i.e., the rate of inactivation is zero) regardless of whether it is in solution or bound to a scaffold as could be the case in a mutant kinase; no spontaneous activation occurs on the time scale of our simulation because the energy required to remove a phosphate group in the absence of an enzyme is very large in biological contexts.

We calculated θ for situations where scaffolds enhance (SI Fig. 9 *a* and *c*) and where they inhibit (SI Fig. 9 *b* and *d*) signal amplification in the “wild-type” case (Figs. 2 and 3). All other parameters are the same as those used in Figs. 2 *a* and *b* and 3 *c* and *d*, and scaffold-bound kinases cannot act on their targets that remain in solution.

We first investigate the situation where kinases are protected from phosphatases only when they are bound to the scaffold. As seen in SI Fig. 9 *a* and *b* qualitative results are identical to their analogous cases in Figs. 2 and 3. Quantitative signal output does, however, change, because the value of N_{scaf} , and hence signal output, increases because some kinases are permanently active when bound to the scaffold.

Now, we consider the situation in which phosphatases do not act on a particular kinase irrespective of whether it is bound to the scaffold or in solution. First, we discuss the case of high constitutive phosphatase activity (SI Fig. 9*c*). For the case where phosphatases cannot act upon the first kinase (A), we find that the qualitative behavior in signal amplitude is the same as that in Fig. 2*b* (SI Fig. 9*c*, diamonds) and scaffolds amplify signals. However, when phosphatases do not act on kinase B (SI Fig. 9*c*, circles), scaffolding makes only a minor difference for the case of high phosphatase activity. In

solution, when the first active kinase (A^*) is protected from phosphatase action, the step involving $C \rightarrow C^*$ is still hindered by the quick deactivation of B^* by phosphatases. Our results imply that the short encounter time for this step on a scaffold allows it to amplify signals in this circumstance. However, when kinase B is protected from phosphatase activity, the step involving $C \rightarrow C^*$ is not hindered by the inactivation of B^* , and the advantage of having a short encounter time becomes less important.

This suggests something counterintuitive; scaffold proteins could potentially inhibit signaling if the final (kinase C) kinase along the cascade is protected from phosphatase interactions. This is observed in SI Fig. 9c (crosses) where kinase C is protected. This effect follows from a consideration of the excess kinases in solution that are never allowed to assemble onto a scaffold because the affinity of a kinase to a scaffold is sufficiently strong so that the kinases do not exchange from the scaffold in the time scale of the simulation. However, such an inhibitory function is eliminated when downstream kinases are allowed to exchange from the scaffold (in reasonable times) as all kinases eventually become permanently activated.

Finally, for low basal phosphatases levels, similar qualitative behavior to that observed in Fig. 3 is seen at low phosphatase activities. For this case, in both the wild-type and kinase-protected scenarios (SI Fig. 9d), the inhibitory effects of the scaffold dominate provided that scaffold bound kinases cannot interact with their substrates in solution and the exchange rate from the scaffold is not too fast.

1. Harding A, Tian TH, Westbury E, Frische E, Hancock JF (2005) *Curr Biol* 15:869-873.
2. Arrio-Dupont M, Foucault G, Vacher M, Devaux PF, Cribier S (2000) *Biophys J* 78:901-907.
3. Ferrell JE (1996) *Trends Biochem Sci* 21:460-466.

4. Ghaemmaghami S, Huh W, Bower K, Howson RW, Belle A, Dephoure N, O'Shea EK, Weissman JS (2003) *Nature* 425:737-741.
5. Goldbeter A, Koshland DE (1981) *Proc Natl Acad Sci USA* 78:6840-6844.
6. Burack WR, Sturgill TW (1997) *Biochemistry* 36:5929-5933.
7. Leibler L (1980) *Macromolecules* 13:1602-1617.
8. Stillinger FH, Bennaïm A (1981) *J Chem Phys* 74:2510-2517.
9. McQuarrie DA, S. J (1997) *Physical Chemistry: A Molecular Approach* (Univ Sci Books, Mill Valley, CA).